Supporting Information: Accurate Binding of Sodium and Calcium to a POPC Bilayer by Effective Inclusion of Electronic Polarization

Josef Melcr,[†] Hector Martinez-Seara,[†] Ricky Nencini,[†] Jiří Kolafa,[‡] Pavel Jungwirth,[†,¶] and O. H. Samuli Ollila[*,†,§]

[†]*Institute of Organic Chemistry and Biochemistry, Academy of Sciences of the Czech Republic, Prague 6, Czech Republic*

[‡]*Department of Physical Chemistry, Institute of Chemical Technology, Prague 6, Czech Republic*

[¶]*Department of Physics, Tampere University of Technology, P.O. Box 692, FI-33101 Tampere, Finland*

[§]*Institute of Biotechnology, University of Helsinki*

E-mail: samuli.ollila@helsinki.fi

S1 Simulation details

Table S1: Simulation parameters

simulation property	parameter
time-step	2 fs
equilibration time	100 ns
total simulation time	300 ns
temperature	313 K
thermostat	v-rescale[1]
barostat	Parrinello-Rahman, semi-isotropic[2]
long-range electrostatics	PME[3]
cut-off scheme	Verlet[4]
Coulomb and VdW cut-off	1.0 nm
constraints	LINCS, only hydrogen atoms[5]
constraints for water	SETTLE[6]

OpenMM simulations were run with 4 fs time step using 4 times heavier hydrogen atoms (mass subtracted from neighbouring atoms).

S2 Area per molecule and calcium binding with different water models

Table S2: Area per lipid (APL) from different models of POPC with no ions

model	APL (Å^2)	Temperature [K]
Lipid14	65.1± 0.6	300
Lipid14[7]	65.6± 0.5	303
ECC-POPC		
SPC/E	63.2± 0.6	300
SPC/E	65.1± 0.6	313
OPC3	62.2± 0.6	300
OPC3	64.2± 0.6	313
OPC	64.4± 0.6	313
TIP4p/2005	66.8± 0.6	313
TIP3p	66.2± 0.6	313
TIP3p-FB	64.8± 0.6	313
TIP4p-FB	65.6± 0.6	313
experiment[8]	62.7± 1.3	293
	64.3± 1.3	303
	67.3± 1.3	323
	68.1± 1.4	333

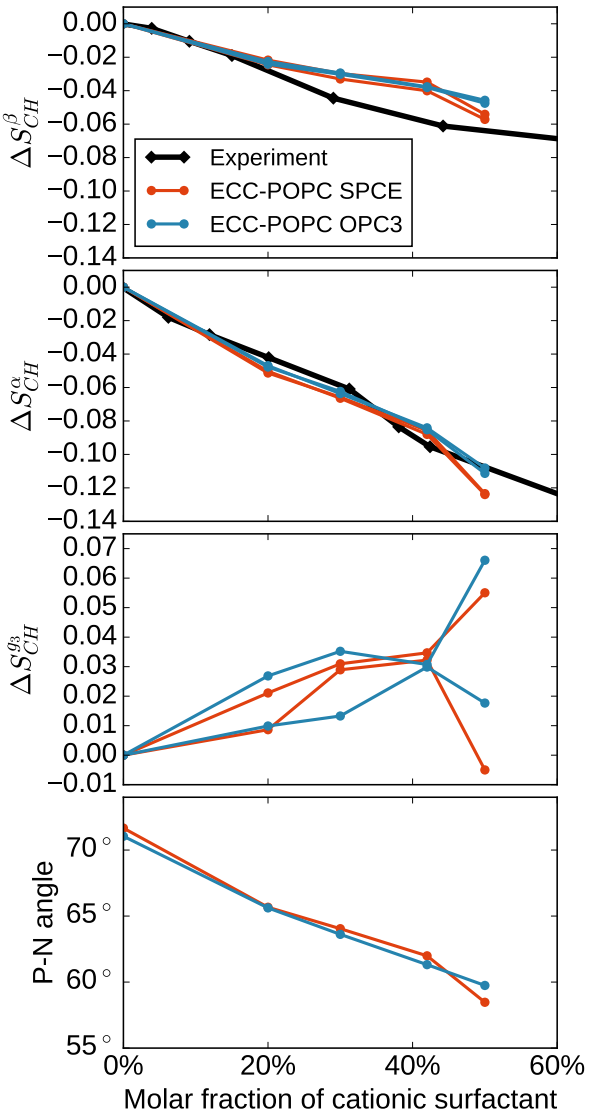

Figure S1: Changes of head group and glycerol carbon g_3 order parameters, and P-N vector orientation of POPC bilayer as a function of a molar fraction of the cationic surfactant dihexadecyldimethylammonium in a POPC bilayer from simulations with different water models (OPC3,[9] SPC/E[10]) and experiments[11] at 313 K.

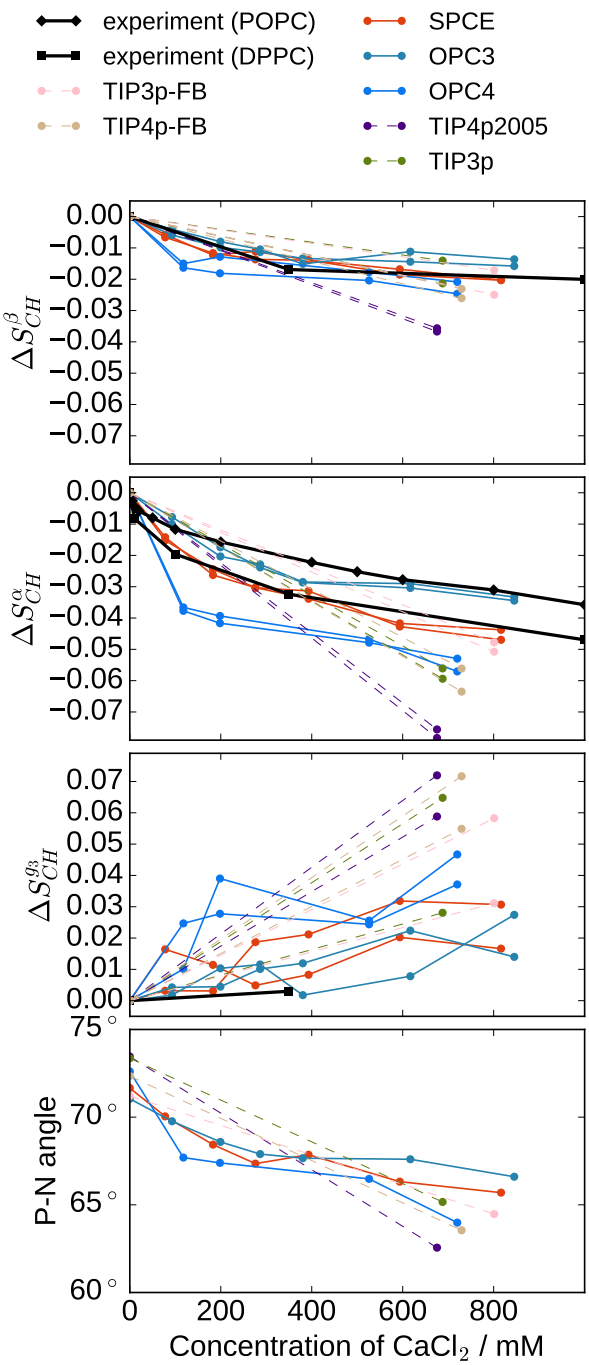

Figure S2: Changes of head group and glycerol carbon g_3 order parameters, and P-N vector orientation of POPC bilayer as a function of $CaCl_2$ concentrations in bulk (C_{ion}) from ECC-POPC simulations at 313K with different water models (SPC/E,[10] OPC,[12] OPC3,[9] TIP3P,[13] TIP3p-FB and TIP4p-FB,[14] and TIP4p/2005[15]) together with experimental data (DPPC (323 K)[16] and POPC (313 K)[17]). Ion concentrations (C_{ion}) are calculated from the cation number density C_{np} at the farthest point from the lipid bilayer in the aqueous phase as [ion]=C_{np}/0.602.

S3 Electronic continuum correction applied to CHARMM36 model

To demonstrate that the ECC method can also be applied to other models than Lipid14, we scaled the charges and Lennard-Jones radii of headgroup, glycerol backbone and carbonyl atoms of the CHARMM36 model of POPC.[18] We used the same scaling factors optimized for Lipid14 in the main text, i.e., 0.8 for charges and 0.89 for Lennard-Jones radii. In Figs. S3 and S4 we show changes of the headgroup order parameters as functions of added ions and number density profiles along membrane normal for our ECC-CHARMM36 model, together with the CHARMM36 model[19,20] and experiments.[16,17] As shown previously,[19] the binding of Ca^{2+} is significantly overestimated in CHARMM36 simulations where no explicit repulsive Ca^{2+}–oxygen Lennard-Jones parameters are included. In ECC-CHARMM36 simulations, the Ca^{2+} binding affinity is reduced substantially (Fig. S4), and the headgroup order parameter response to the added $CaCl_2$ is in a better agreement with experiments than for the original CHARMM36 model (Fig. S3). Fig. S5 also shows faster equilibration times for Ca^{2+} binding in the ECC-CHARMM36 model than in the original CHARMM36. Both results are in line with the findings described in the main text.

In conclusion, applying ECC to CHARMM36 simulation improved the ion binding affinity to a lipid bilayer, despite we directly applied the scaling factors optimized for Lipid14 without further optimizations. Also, the area per molecule in the ECC-CHARMM36 simulation without ions (61 Å^2) is only slightly lower than the experimental value (64.3 Å^2).[8] The optimal scaling factors for CHARMM36 are expected to be somewhat different than for Lipid14 because the initial partial charges are not the same in the two models. Our results indicate that the performance of ion binding in ECC-CHARMM36, and probably in other lipid models as well, could be further improved by finding the optimal values for the partial charges and Lennard-Jones radii.

It should be noted that the CHARMM36 simulation used here uses the original paramter

as in our previous study.[19,20] Currently (February 2018), specific interaction parameters between calcium and oxygen[21] have been introduced in CHARMM-GUI[22] to reduce the binding of calcium to lipid bilayers. The further discussion of these changes that dramatically reduce the calcium binding to levels similar to sodium is beyond the scope of this work.

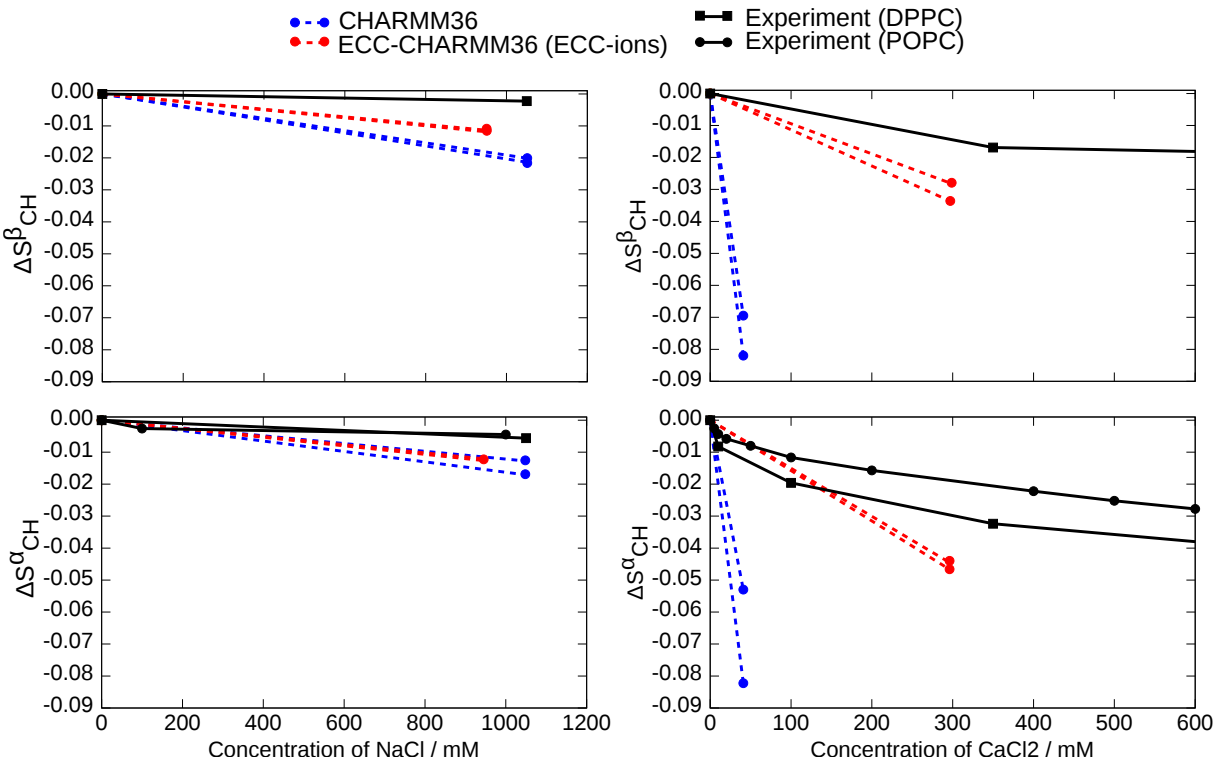

Figure S3: Changes of the headgroup order parameters as a function of NaCl (left) and $CaCl_2$ (right) from simulations with CHARMM36,[18] simulations with ECC-CHARMM36 parameters and experiments.[16,17] CHARMM36 force field parameters for simulations with and without NaCl were taken from CHARMM-GUI.[22] These were ran 320 ns and 280 ns, respectively, and the first 100 ns was omitted from the analysis. Results for CHARMM36 with $CaCl_2$ were calculated from the last 100 ns from the data available at Ref. 20. ECC-CHARMM36 simulations with NaCl and $CaCl_2$ were ran 260 ns and 600 ns, respectively, and the first 100 ns were omitted from the analysis. Sodium, calcium, and chloride ions were modeled as ECC-ions in these simulations with parameters from Refs. 23,24. All the other simulation parameters in simulations in this figure were equal to the available dataset at Ref. 20. The temperature in all simulations was set to 310 K. The simulation data is available at Refs. 25–29.

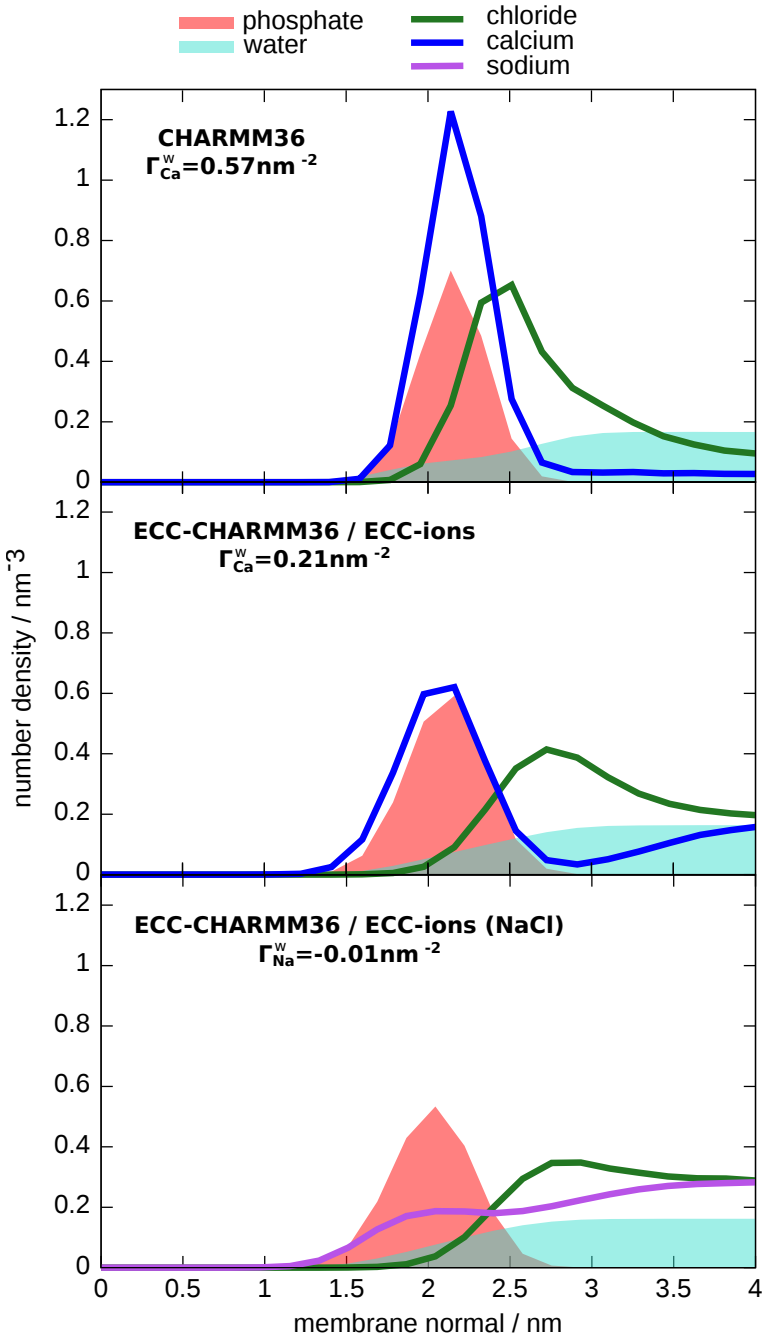

Figure S4: Number density profiles along membrane normal from CHARMM36[18] and ECC-CHARMM36 models with NaCl and $CaCl_2$. The values for the relative surface excess are also shown. Simulation details are as in Fig. S3.

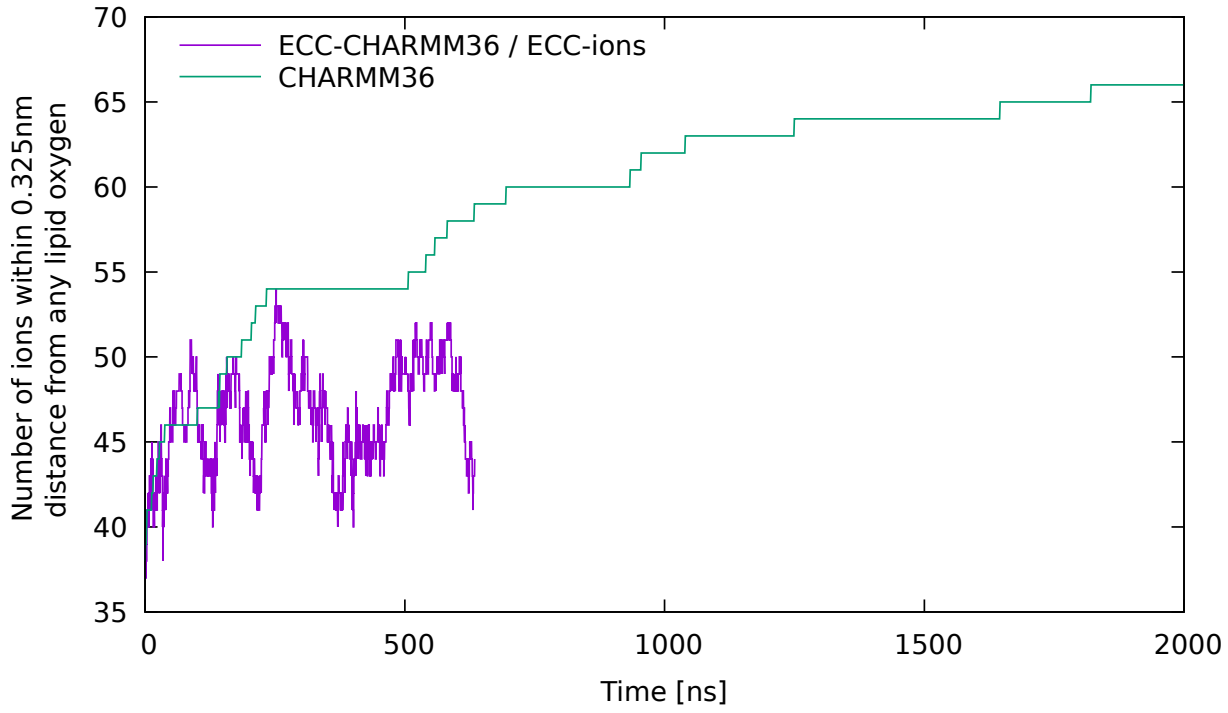

Figure S5: Number of bound Ca^{2+} during simulations. The data for CHARMM36 is taken directly from Refs. 19,20,30

S4 Sodium binding to POPC with the glycerol carbon g_3 order parameters and the head group orientation

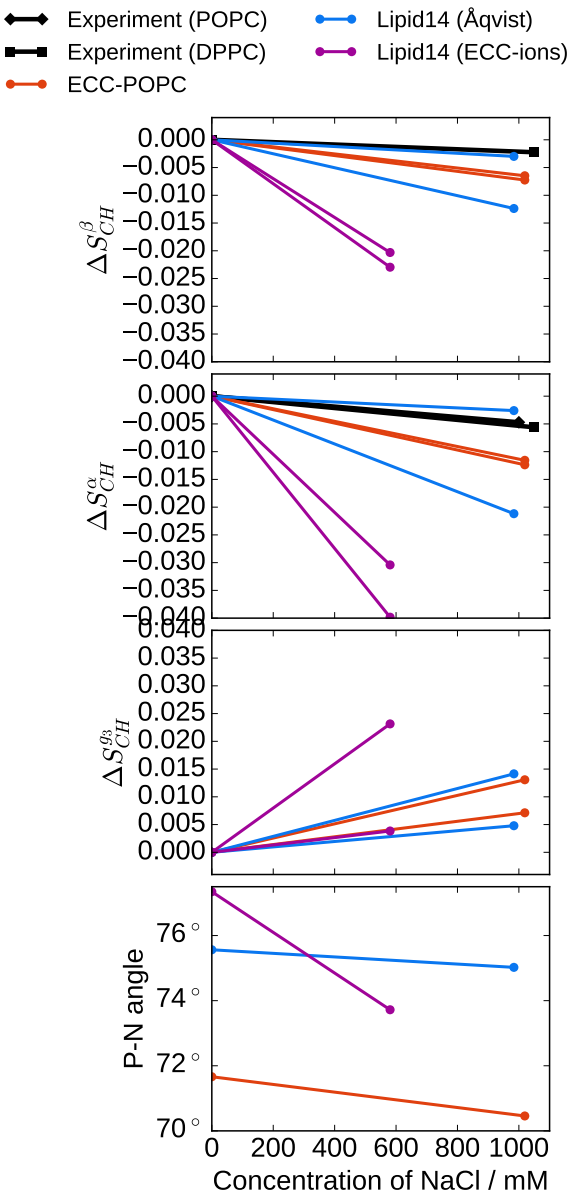

Figure S6: Changes of head group and glycerol carbon g_3 order parameters, and the P-N vector orientation of POPC bilayer as a function of NaCl concentrations in bulk (C_{ion}) from simulations with different force fields at 313 K together with experimental data (DPPC (323 K)[16] and POPC (313 K)[17]). Simulation data with Lipid14 and Åqvist ion parameters at 293 K is taken directly from Refs. 19,31,32.

S5 Ternary complex model in simulations

The NMR data about PC headgroup order parameters and atomic absorption spectroscopy data were previously best explained using a ternary complex binding model.[17] In this model, one calcium is assumed to form complexes with two lipids, i.e. with the binding stoichiometry of 1 Ca^{2+}:2 POPC. The model predicts a linear relationship between quantities C_b and $\sqrt{C_b/C_I}$, where C_b is the mole fraction of bound Ca^{2+} per POPC and C_I is the concentration of free cations at the plane of ion binding.[17] Experimentally detemined C_b from NMR measurements and atomic absorption spectroscopy together with C_I calculated from the Poisson-Boltzmann equation gave a good agreement with the predictions of the ternary complex model.[17]

To compare ECC-POPC simulations to the ternary complex model, we calculated C_b from simulations (as defined in the main text), and C_I from the minimum $CaCl_2$ concentration at membrane-water interface, locating around 2.6 nm from the membrane center in the density profiles in Fig. 5 in the main text.

The results from simulations are shown in Fig. S7 together with the line fitted to experimental data by Altenbach and Seelig.[17] Both results are in agreement with the prediction of the ternary complex model. The small discrepancy between the results from experiments and simulations probably arise from difference in the evaluation of the concentrations and inaccuracy of Poisson-Boltzmann theory for divalent cations like Ca^{2+}.[33] In conclusion, the results suggest that the almost equal probabilities for Ca^{2+} to form complexes with one to three lipids detailed in the main text is in line with an averaged interpretation of the experimental observations which supported the ternary complex model.

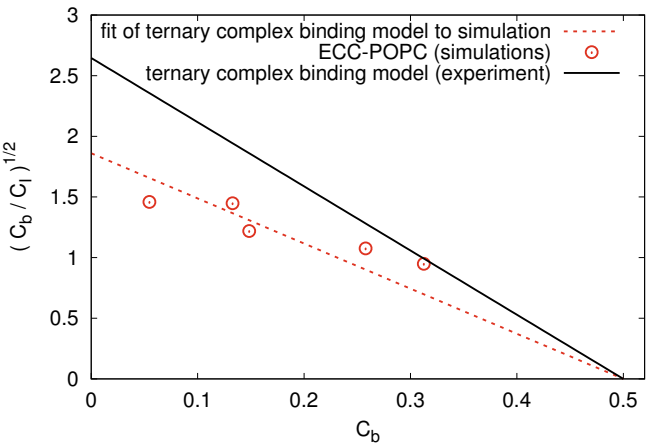

Figure S7: Fits of experimental[17] and ECC-POPC simulation data to the prediction of the ternary complex model.

S6 Histograms of residence times

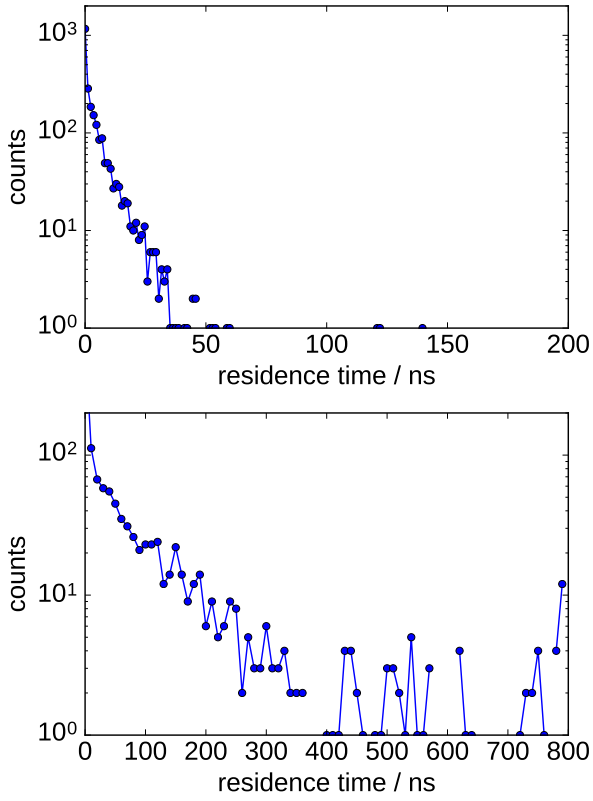

Figure S8: Histograms of residence times of Ca^{2+} in a POPC bilayer from ECC-POPC (top) and CHARMM36 (bottom) simulations with ECC-ions. Both simulations had the same concentration of $CaCl_2$ respect to water (C'_{ion}= 450 mM). CHARMM36 simulation was directly taken from Refs. 34,35. Scales of x-axes represent the lengths of the simulations used for analysis. In ECC-POPC simulation, 90% of the residence times are shorter than 60 ns, with the longest observed residence time being 141 ns, which is well below the total length of the simulation (200 ns). This is, however not the case in CHARMM36 simulation, where residence times of several calcium cations are apparently limited by the length of the simulation. Less than 60% of the residence times are shorter than the half of the simulation length (400 ns) in CHARMM36 simulation.

S7 Comparison between Gromacs and openMM

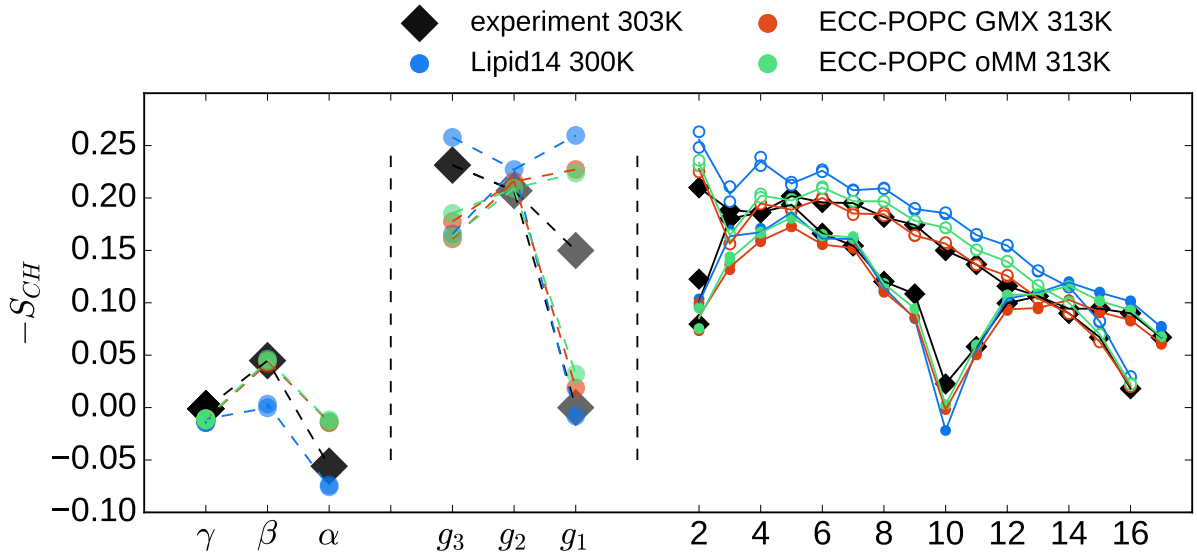

Figure S9: Order parameters of POPC head group, glycerol backbone and acyl chains from Lipid14[7] and ECC-POPC simulations ran with GROMACS 5.1.4[36] and openMM 7[37] together with experiments.[38] The size of the markers for the head group order parameters correspond to the error estimate ±0.02 for experiments,[39,40] while the error estimate for simulations is ±0.005. The size of the points for acyl chains are decreased by a factor of 3 to improve the clarity of the plot.

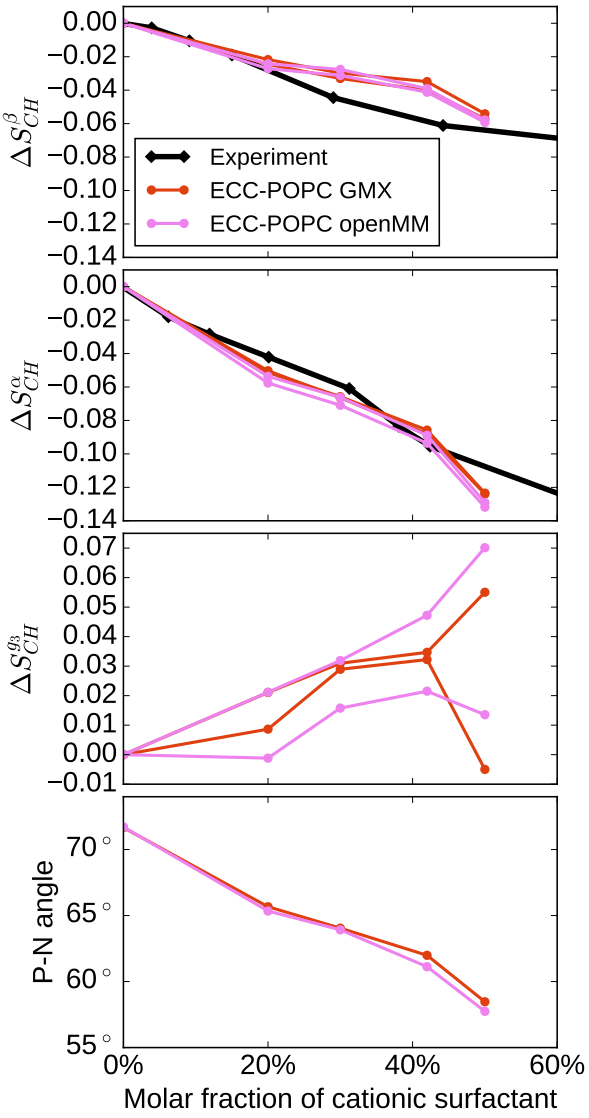

Figure S10: Changes of headgroup and glycerol carbon g_3 order parameters, and P-N vector orientation as a function of a molar fraction of the cationic surfactant dihexadecyldimethylammonium in a POPC bilayer from simulations with the ECC-POPC model simulated with GROMACS 5.1.4[36] and openMM 7[37] compared with the experimental values from.[11] The size of the markers for the head group order parameters correspond to the error estimate ±0.02 for experiments,[39,40] while the error estimate for simulations is ±0.005.

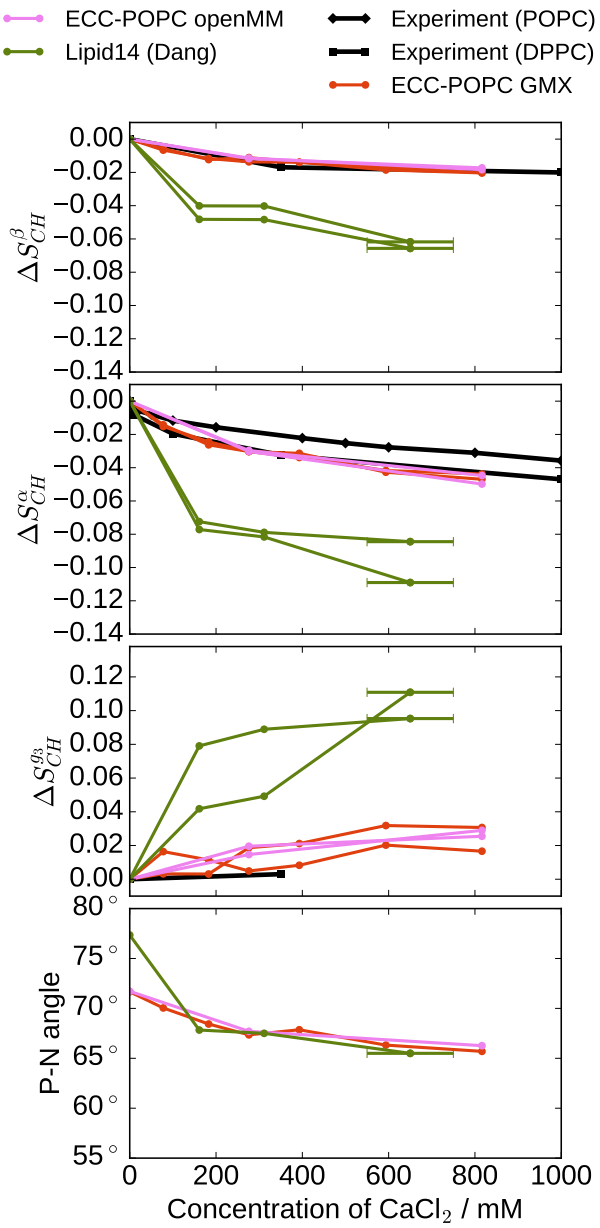

Figure S11: Changes of the head group and glycerol carbon g_3 order parameters, and P-N vector orientation of a POPC bilayer as a function of the $CaCl_2$ concentration in bulk (C_{ion}) from Lipid14[7] and ECC-POPC simulations ran with GROMACS 5.1.4[36] and openMM 7[37] at 313 K together with experiments (DPPC (323 K)[16] and POPC (313 K)[17]). Bulk concentrations from simulations are calculated from the farthest point from the lipid bilayer in the aqueous phase with an error estimate of 10 mM.

S8 Electrostatic potential of lipid bilayer

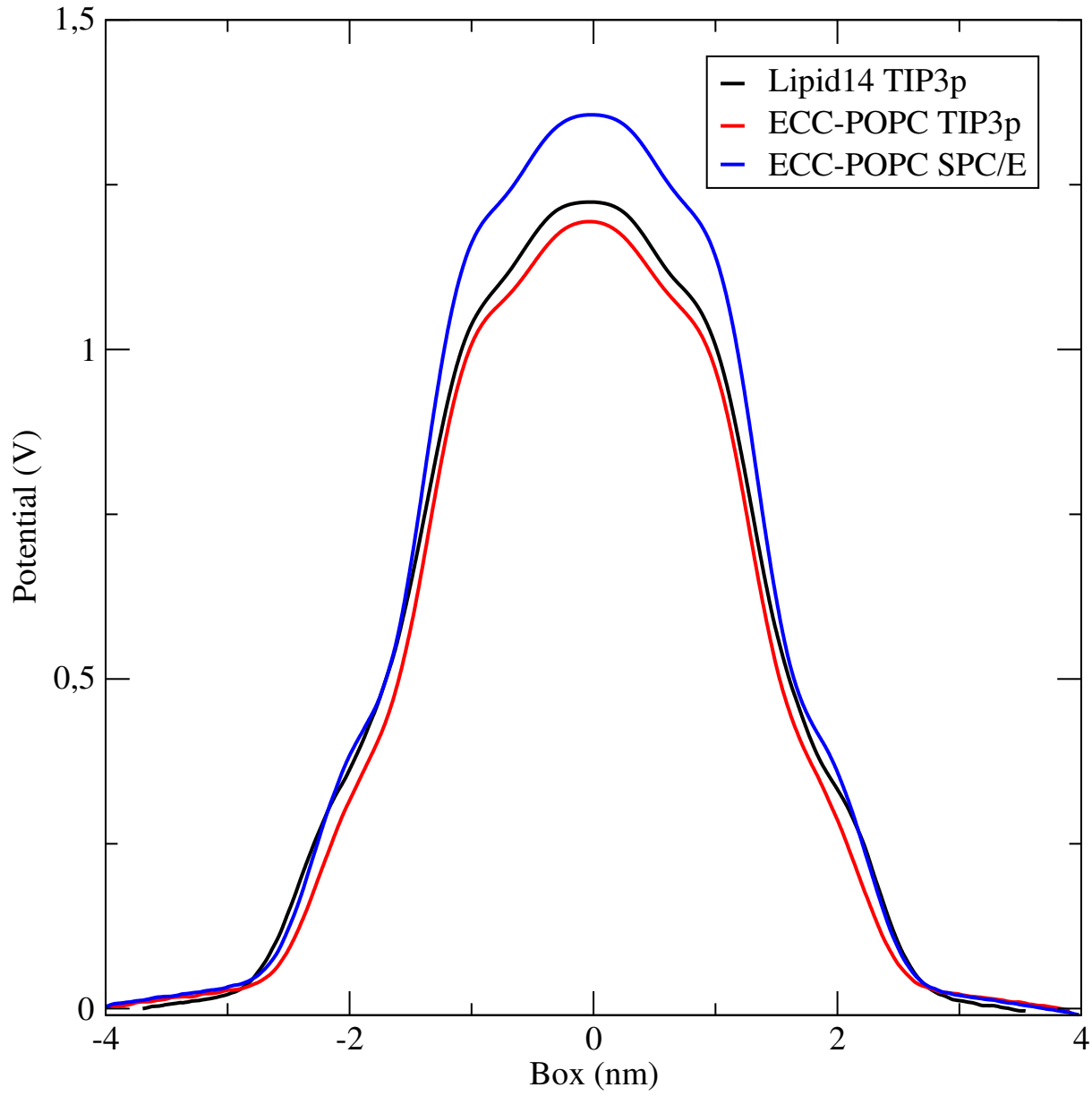

Figure S12: Electrostatic potential calculated by evaluating the double integral of the charge density using *gmx potential* tool from Gromacs package.[41] Comparing the Lipid14 and ECC-POPC simulations with TIP3P water model reveals that applying ECC to the headgroup and glycerol backbone charges slightly decreases the dipole potential inside the bilayer. On the other hand, ECC-POPC simulation with SPC/E water model has larger dipole pontential than with TIP3P. The stronger dependence of water model is expected as the dipole potential mainly originates from orientation of water molecules.[42]

S9 Binding of potassium to ECC-POPC lipid bilayer

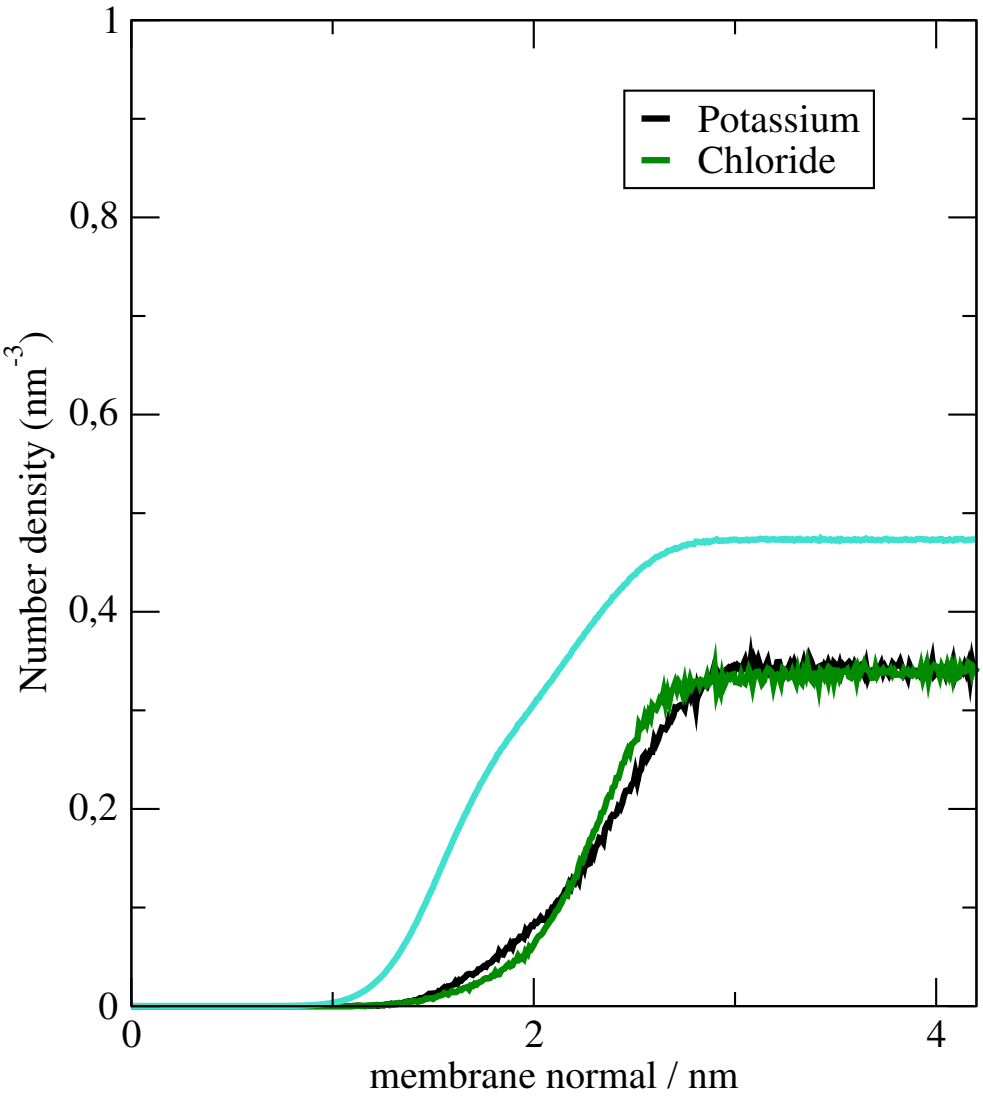

Figure S13: Number density profiles of K^+, Cl^- and water along membrane normal axis from ECC-POPC simulation with KCl (C'_{ion}=1000mM, simulation parameters as in Table S1). Parameters for ions are taken from Ref. 43. In consistent with figure 5 in the main text, the density profiles of ions and water are divided with 2 and 200, respectively. Similarity of potassium and chloride curves together with the bulk concentrations indicate lower binding affinity for potassium than for sodium (Fig. 5 in the main text). Since this is in line with wide range of experimental data,[44–46] we conclude that the ECC-POPC model reproduces the correct binding affinity also for potassium. In line with the low binding affinity, the headgroup order parameters were not affected by the presense of KCl in simulations. The order parameter data is not shown because we are not aware of experimental data for PC headgroup order parameters as a function of KCl concentration.

References

(1) Bussi, G.; Donadio, D.; Parrinello, M. Canonical sampling through velocity rescaling. *J. Chem. Phys.* **2007**, *126*, 014101.

(2) Parrinello, M.; Rahman, A. Polymorphic transitions in single crystals: A new molecular dynamics method. *J. Appl. Phys.* **1981**, *52*, 7182–7190.

(3) Darden, T.; York, D.; Pedersen, L. Particle mesh Ewald: An N·log(N) method for Ewald sums in large systems. *J. Chem. Phys.* **1993**, *98*, 10089–10092.

(4) Páll, S.; Hess, B. A flexible algorithm for calculating pair interactions on {SIMD} architectures. *Comput. Phys. Commun.* **2013**, *184*, 2641 – 2650.

(5) Hess, B.; Bekker, H.; Berendsen, H. J. C.; Fraaije, J. G. E. M. LINCS: a linear constraint solver for molecular dynamics simulations. *J. Comput. Chem.* **1997**, *18*, 1463–1472.

(6) Miyamoto, S.; Kollman, P. A. SETTLE: An analytical Version of the SHAKE and RATTLE Algorithm for Rigid Water Models. *J. Comput. Chem* **1992**, *13*, 952–962.

(7) Dickson, C. J.; Madej, B. D.; Skjevik, Ã. A.; Betz, R. M.; Teigen, K.; Gould, I. R.; Walker, R. C. Lipid14: The amber lipid force field. *J. Chem. Theory Comput.* **2014**, *10*, 865–879.

(8) Kučerka, N.; Nieh, M. P.; Katsaras, J. Fluid phase lipid areas and bilayer thicknesses of commonly used phosphatidylcholines as a function of temperature. *Biochim. Biophys. Acta* **2011**, *1808*, 2761–2771.

(9) Izadi, S.; Onufriev, A. V. Accuracy limit of rigid 3-point water models. *J. Chem. Phys.* **2016**, *145*, 074501.

(10) Berendsen, H. J. C.; Grigera, J. R.; Straatsma, T. P. The missing term in effective pair potentials. *J. Phys. Chem.* **1987**, *91*, 6269–6271.

(11) Scherer, P. G.; Seelig, J. Electric charge effects on phospholipid headgroups. Phosphatidylcholine in mixtures with cationic and anionic amphiphiles. *Biochemistry* **1989**, *28*, 7720–7728.

(12) Izadi, S.; Anandakrishnan, R.; Onufriev, A. V. Building water models: A different approach. *J. Phys. Chem. Lett.* **2014**, *5*, 3863–3871.

(13) Jorgensen, W. L.; Chandrasekhar, J.; Madura, J. D.; Impey, R. W.; Klein, M. L. Comparison of simple potential functions for simulating liquid water. *J. Chem. Phys* **1983**, *79*, 926–935.

(14) Wang, L. P.; Martinez, T. J.; Pande, V. S. Building force fields: An automatic, systematic, and reproducible approach. *Phys. Chem. Lett.* **2014**, *5*, 1885–1891.

(15) Abascal, J. L.; Vega, C. A general purpose model for the condensed phases of water: TIP4P/2005. *J. Chem. Phys.* **2005**, *123*, 234505.

(16) Akutsu, H.; Seelig, J. Interaction of metal ions with phosphatidylcholine bilayer membranes. *Biochemistry* **1981**, *20*, 7366–7373.

(17) Altenbach, C.; Seelig, J. Calcium binding to phosphatidylcholine bilayers as studied by deuterium magnetic resonance. Evidence for the formation of a calcium complex with two phospholipid molecules. *Biochemistry* **1984**, *23*, 3913–3920.

(18) Klauda, J. B.; Venable, R. M.; Freites, J. A.; O'Connor, J. W.; Tobias, D. J.; Mondragon-Ramirez, C.; Vorobyov, I.; Jr, A. D. M.; Pastor, R. W. Update of the CHARMM All-Atom Additive Force Field for Lipids: Validation on Six Lipid Types. *J. Phys. Chem. B* **2010**, *114*, 7830–7843.

(19) Catte, A.; Girych, M.; Javanainen, M.; Loison, C.; Melcr, J.; Miettinen, M. S.; Monticelli, L.; Maatta, J.; Oganesyan, V. S.; Ollila, O. H. S. et al. Molecular electrometer

and binding of cations to phospholipid bilayers. *Phys. Chem. Chem. Phys.* **2016**, *18*, 32560–32569.

(20) Javanainen, M. POPC @ 310K, 450 mM of CaCl_2. Charmm36 with default Charmm ions. 2016; http://dx.doi.org/10.5281/zenodo.51185.

(21) Kim, S.; Patel, D.; Park, S.; Slusky, J.; Klauda, J.; Widmalm, G.; Im, W. Bilayer Properties of Lipid A from Various Gram-Negative Bacteria. *Biophys. J.* **2016**, *111*, 1750 – 1760.

(22) Lee, J.; Cheng, X.; Swails, J. M.; Yeom, M. S.; Eastman, P. K.; Lemkul, J. A.; Wei, S.; Buckner, J.; Jeong, J. C.; Qi, Y. et al. CHARMM-GUI Input Generator for NAMD, GROMACS, AMBER, OpenMM, and CHARMM/OpenMM Simulations Using the CHARMM36 Additive Force Field. *J. Chem. Theory Comput.* **2016**, *12*, 405–413.

(23) Martinek, T.; Duboué-Dijon, E.; Timr, S.; Mason, P. E.; Baxová, K.; Fischer, H. E.; Schmidt, B.; Pluhařová, E.; Jungwirth, P. Calcium ions in aqueous solutions: Accurate force field description aided by ab initio molecular dynamics and neutron scattering. *J. Chem. Phys.* **2018**, *148*, 222813.

(24) Pluhařová, E.; Fischer, H. E.; Mason, P. E.; Jungwirth, P. Hydration of the chloride ion in concentrated aqueous solutions using neutron scattering and molecular dynamics. *Mol. Phys.* **2014**, *112*, 1230–1240.

(25) Nencini, R. Simulation data for CHARMM36 POPC bilayer, 100 lipids/leaflet, 310K, GROMACS 5.1.4. 2018; https://doi.org/10.5281/zenodo.1198158.

(26) Nencini, R. Simulation data for CHARMM36 POPC bilayer, 100 lipids/leaflet, 940 mM NaCl, 310K, GROMACS 5.1.4. 2018; https://doi.org/10.5281/zenodo.1198454.

(27) Nencini, R. Simulation data for ECC-CHARMM36 POPC bilayer, 100 lipids/leaflet, 310K, GROMACS 5.1.4. 2018; https://doi.org/10.5281/zenodo.1198213.

(28) Nencini, R. Simulation data for ECC-CHARMM36 POPC bilayer, 100 lipids/leaflet, 940 mM NaCl, 310K, GROMACS 5.1.4. 2018; https://doi.org/10.5281/zenodo.1198463.

(29) Nencini, R. Simulation data for ECC-CHARMM36 POPC bilayer, 100 lipids/leaflet, 450 mM CaCl2, 310K, GROMACS 5.1.4. 2018; https://doi.org/10.5281/zenodo.1198338.

(30) Catte, A.; Girych, M.; Javanainen, M.; Loison, C.; Melcr, J.; Miettinen, M. S.; Monticelli, L.; Määttä, J.; Oganesyan, V. S.; Ollila, O. H. S. et al. NMR-Lipids/lipid_ionINTERACTION: Final submission to Physical Chemistry Chemical Physics. 2016; https://doi.org/10.5281/zenodo.167370.

(31) Girych, M.; Ollila, O. H. S. POPC_AMBER_LIPID14_Verlet. 2015; http://dx.doi.org/10.5281/zenodo.30898.

(32) Girych, M.; Ollila, O. H. S. POPC_AMBER_LIPID14_NaCl_1Mol. 2015; http://dx.doi.org/10.5281/zenodo.30865.

(33) Andelman, D. *Handbook of biological physics*; Elsevier Science, 1995; Vol. 1; Chapter 12, pp 603–642.

(34) Javanainen, M.; Melcrová, A.; Magarkar, A.; Jurkiewicz, P.; Hof, M.; Jungwirth, P.; Martinez-Seara, H. Two cations, two mechanisms: interactions of sodium and calcium with zwitterionic lipid membranes. *Chem. Commun.* **2017**, *53*, 5380–5383.

(35) Javanainen, M. POPC with varying amounts of cholesterol, 450 mM of CaCl_2. Charmm36 with ECC-scaled ions. 2017; https://doi.org/10.5281/zenodo.259376.

(36) Abraham, M. J.; Murtola, T.; Schulz, R.; Páll, S.; Smith, J. C.; Hess, B.; Lindah, E. Gromacs: High performance molecular simulations through multi-level parallelism from laptops to supercomputers. *SoftwareX* **2015**, *1-2*, 19–25.

(37) Eastman, P.; Swails, J.; Chodera, J. D.; McGibbon, R. T.; Zhao, Y.; Beauchamp, K. A.; Wang, L.-P.; Simmonett, A. C.; Harrigan, M. P.; Stern, C. D. et al. OpenMM 7: Rapid development of high performance algorithms for molecular dynamics. *PLOS Comput. Biol.* **2017**, *13*, e1005659.

(38) Ferreira, T. M.; Coreta-Gomes, F.; Ollila, O. H. S.; Moreno, M. J.; Vaz, W. L. C.; Topgaard, D. Cholesterol and POPC segmental order parameters in lipid membranes: solid state 1H-13C NMR and MD simulation studies. *Phys. Chem. Chem. Phys.* **2013**, *15*, 1976–1989.

(39) Botan, A.; Favela-Rosales, F.; Fuchs, P. F. J.; Javanainen, M.; Kanduč, M.; Kulig, W.; Lamberg, A.; Loison, C.; Lyubartsev, A.; Miettinen, M. S. et al. Toward atomistic resolution structure of phosphatidylcholine headgroup and glycerol backbone at different ambient conditions. *J. Phys. Chem. B* **2015**, *119*, 15075–15088.

(40) Ollila, O. S.; Pabst, G. Atomistic resolution structure and dynamics of lipid bilayers in simulations and experiments. *Biochim. Biophys. Acta* **2016**, *1858*, 2512 – 2528.

(41) Abraham, M.; van der Spoel, D.; Lindahl, E.; Hess, B.; the GROMACS development team, GROMACS user manual version 5.0.7. 2015.

(42) Gawrisch, K.; Ruston, D.; Zimmerberg, J.; Parsegian, V.; Rand, R.; Fuller, N. Membrane dipole potentials, hydration forces, and the ordering of water at membrane surfaces. *Biophys. J.* **1992**, *61*, 1213 – 1223.

(43) Mason, P. E.; Wernersson, E.; Jungwirth, P. Accurate Description of Aqueous Carbonate Ions: An Effective Polarization Model Verified by Neutron Scattering. *J. Phys. Chem. B* **2012**, *116*, 8145–8153.

(44) Eisenberg, M.; Gresalfi, T.; Riccio, T.; McLaughlin, S. Adsorption of monovalent cations to bilayer membranes containing negative phospholipids. *Biochemistry* **1979**, *18*, 5213–5223.

(45) Binder, H.; Zschörnig, O. The effect of metal cations on the phase behavior and hydration characteristics of phospholipid membranes. *Chem. Phys. Lipids* **2002**, *115*, 39 – 61.

(46) Klasczyk, B.; Knecht, V.; Lipowsky, R.; Dimova, R. Interactions of alkali metal chlorides with phosphatidylcholine vesicles. *Langmuir* **2010**, *26*, 18951–18958.